

GROWTH OF CLAY MINERALS IN NATURAL AND SYNTHETIC GLASSES

KAZUE TAZAKI,¹ W. S. FYFE,² AND S. J. VAN DER GAAST³

¹ Department of Geology, Shimane University, Nishikawatsu
Matsue, Shimane, Japan 690

² Department of Geology, University of Western Ontario
London, Ontario N6A 5B7, Canada

³ Netherland Institute for Sea Research, P.O. Box 59
1790 AB Den Burg, Texel, The Netherlands

Abstract—High-resolution transmission electron microscopy (HRTEM) has shown regions of crystallites within noncrystalline matrices of three types of glass (volcanic glass, alkalic igneous glass, and synthetic, nuclear-waste-form glass). The volcanic glass fragments showed domains having 3-Å spacings. About 30% of the fragments of this glass showed localized lattice images, having spacings of 5, 7, 8, 10, 13, 14, 16, 19, and 20 Å, which also contain regular fringes having 3.3-Å separations. In the alkalic igneous glass fragments 3-Å domain structures were also noted as were localized lattice images having 7- and 12.5-Å spacings. Well-developed hollow spheres of primitive clays were present in both the volcanic and alkalic igneous glasses. Synthetic, nuclear-waste-form glass, fused at 1400°C and annealed at 550°C, showed locally ordered regions having 3.3-Å spacings. Low-angle X-ray powder diffraction showed major reflections at 8.5, 15–16, and 19 Å, which agree with some of the HRTEM measurements. These observations of domain structures, localized lattice images, primitive clays, and 14-Å clays in such noncrystalline glass matrices may contribute to an understanding of the growth of clay minerals. Such domains can apparently trigger the growth of clay products on the glass substrate.

Key Words—Crystallization, Domain structure, Glass, High-resolution transmission electron microscopy, Noncrystalline, Primitive clay.

INTRODUCTION

Glasses (amorphous or noncrystalline materials) are important constituents of rocks, soils, and marine sediments and of some proposed nuclear-waste forms. The glasses generally coexist with clay minerals in these systems. It has long been recognized that many clay minerals crystallize from noncrystalline precursors by complex adsorption, solution, and precipitation processes. Considerable research has been devoted to the study of the formation of clay minerals in volcanic glass. Much of the halloysite formed from volcanic ash and glass occurs in the form of spherical aggregates (Tazaki, 1976, 1978, 1979; Eggleton and Buseck, 1980). Noncrystalline, hollow-packed spheres have been described as precursors to crystalline clay minerals during the hydration of feldspar and some volcanic glasses (Eggleton and Keller, 1982; Tazaki, 1986; Tazaki and Fyfe, 1985, 1987a, 1987b; Eggleton, 1987). Few studies have been made, however, on the growth of clay minerals in natural and synthetic glasses using high-resolution electron microscopical techniques, and primitive clays themselves have not previously been observed. The present study examined three types of glass (volcanic glass, alkalic igneous glass, and synthetic, nuclear-waste-form glass) using high-resolution transmission electron microscopy (HRTEM) and reports on the formation of regions of crystallite in truly noncrystalline glass matrices. The HRTEM results

contribute towards an understanding of the growth of primitive clay minerals in both natural and synthetic glasses.

MATERIALS AND METHODS

Volcanic glass

Palmer *et al.* (1988) described the widespread occurrence of glass materials in volcanic rocks from Michipicoten Island, Lake Superior, Canada, having an age of about 1.1 Ga. Electron microprobe analyses of the Precambrian glasses showed 64–67% SiO₂, 0.8–1.0% TiO₂, 11–15% Al₂O₃, 1.9–3.6% FeO, 2.5–4.3% CaO, 2.9–5.0% Na₂O, 1.2–1.4% K₂O, and trace amounts of Cr₂O₃, MnO, and MgO (Palmer *et al.*, 1988). An X-ray powder diffractogram, using Ni-filtered Cu radiation, of the whole rock showed a broad enhancement of background at 18°–37°2 θ . Plagioclase and clinopyroxene peaks were also present.

Alkalic igneous glass

The whole rock samples from an alkaline igneous complex, dated at 81 Ma, from Ilha Bela, southern Brazil, contained 64–67% SiO₂, 0.2–0.4% TiO₂, 17–18% Al₂O₃, 1–3% Fe₂O₃, 0.3–0.8% CaO, 6–7% Na₂O, 6% K₂O, and trace amounts of MnO, MgO, and P₂O₅ (Kronberg *et al.*, 1987). Major-element data were obtained by X-ray fluorescence, and trace elements were surveyed using spark-source mass spectroscopy. An

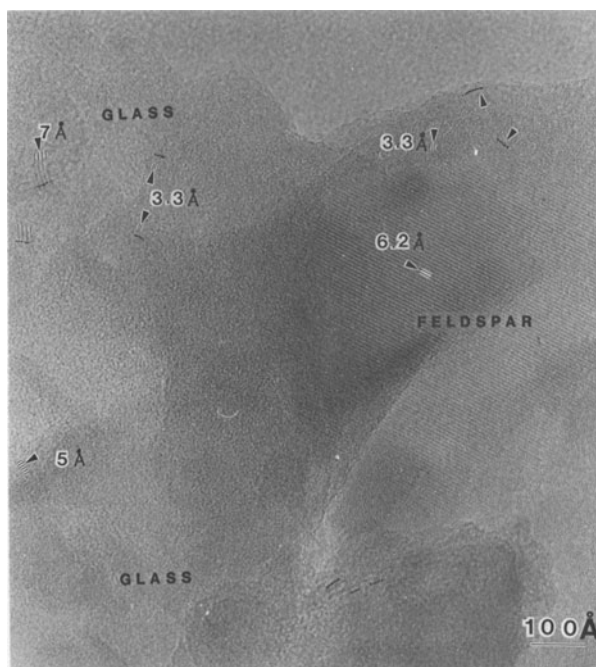


Figure 1. High-resolution transmission electron micrograph of feldspar and glass phases. The 3.3-Å domain structures and what appears to be the early formation of curved structures of 5- and 7-Å spacings can be seen in the crystallite regions in the noncrystalline glass matrix.

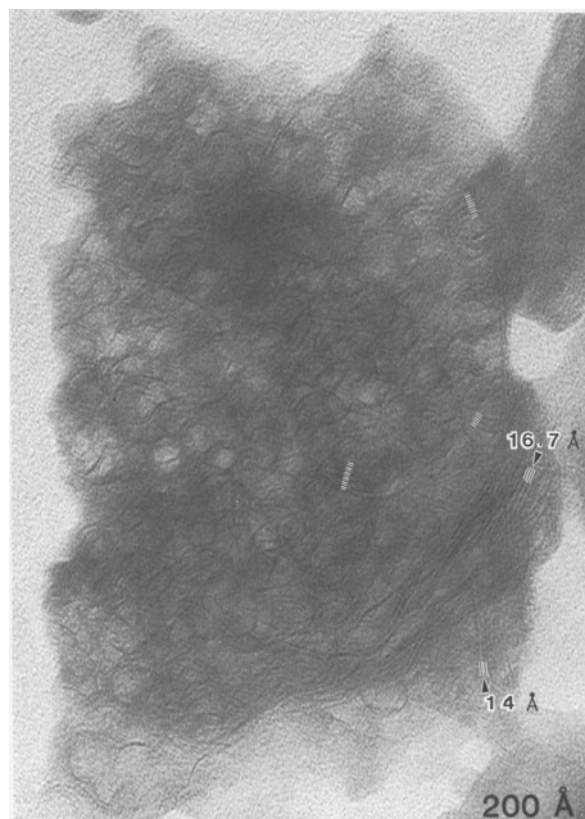


Figure 3. High-resolution transmission electron micrograph of primitive clays on volcanic glass showing 14- and 16.7-Å lattice images.

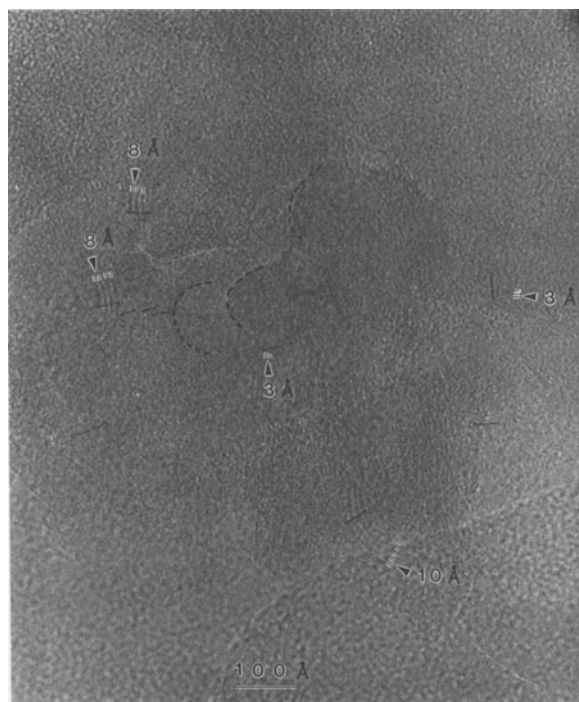


Figure 2. High-resolution transmission micrograph showing early formation of curved structures with 8- and 10-Å spacings and spherical structures showing concentric 3-Å lattice images. 3-Å domain structures are also present.

X-ray powder diffraction pattern of the whole rock showed a broad enhancement of background at 18° – $37^{\circ}2\theta$, suggesting a noncrystalline component. Orthoclase, albite, quartz, pyroxene, and magnetite were also present. Using a $<2\text{-}\mu\text{m}$ size fraction, the transmission electron microscopic examination of perthitic K-feldspar showed evidence for the formation of iron-rich primitive clays having diffuse rings at 4.41, 2.65, 1.56, and 1.38 Å (Tazaki and Fyfe, 1987a, 1987b).

Synthetic, nuclear-waste-form glass

A nuclear-waste-form glass was prepared from mixed oxide powders by fusion at 1400°C in a Pt crucible. To ensure homogeneity, glass pellets from a first fusion were ground and fused a second time. The final glass pellet was annealed at 550°C for 3 hr and cooled to room temperature. The waste-form glass contained 40.0% SiO_2 , 11.1% Fe_2O_3 , 2.0% CaO , 12.9% Na_2O , 3.0% TiO_2 , 9.5% B_2O_3 , 5.0% ZnO , 1.9% ZrO_2 , 2.4% MoO_3 , 3.0% CeO_2 , 3.1% La_2O_3 , and traces of other elements (Zhou *et al.*, 1987). The X-ray powder diffraction pattern of the glass showed only a broad enhancement of background, with a mid-point of the hump at 3.3 Å.

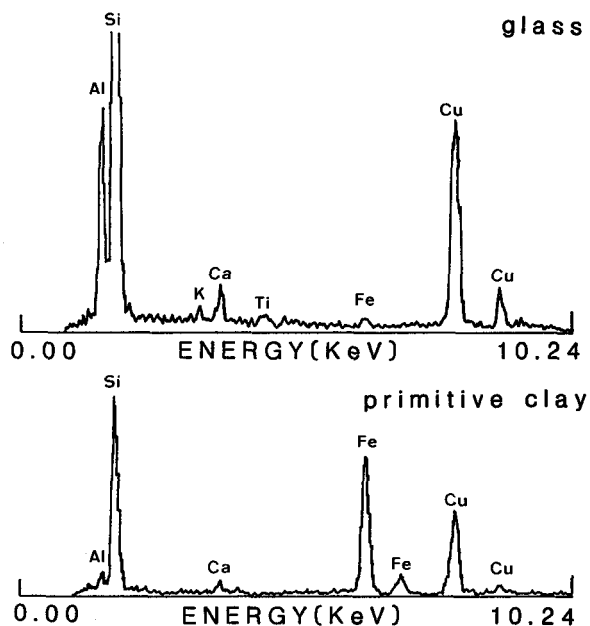


Figure 4. Energy dispersive X-ray spectra data showing relative compositions of glass phase and primitive clay phases. Glass phase contains trace amount of Fe; primitive clay phases show large amount of Fe. Concentrations of Si and Al are less in primitive clay phases. Cu lines are artefacts from specimen support grids.

Analytical methods

The samples were ground with water in a porcelain mortar; the resulting finest fraction was then decanted, and the suspension was allowed to settle. After about 1 hr the supernatant suspension was pipeted and sedimented on a glass slide for an X-ray powder diffractogram (XRD). Grains ($<2\text{-}\mu\text{m}$) were collected by hydraulic elutriation methods and pipeted onto specimen-support micro-grids for transmission electron microscopy (TEM) and scanning TEM (STEM), with energy-dispersive X-ray analysis (EDX) facilities. A JEOL-JEM 100C instrument was used at an accelerating voltage of 100 kV and a JEOL-JEM 4000FX TEM-STEM analytical electron microscope was used at a voltage of 400 kV. Low-angle XRD measurements were made using the technique described by van der Gaast and Vaars (1981) and van der Gaast *et al.* (1986).

The identification of glass was based solely on the isotropic appearance in transmitted light, when examined in thin section. The identification of the non-crystalline component was based on a broad enhancement of background, with a mid-point of the hump at about 3 \AA , when examined in a crushed portion of the whole sample using an X-ray diffractogram. Using a $<2\text{-}\mu\text{m}$ size fraction, TEM techniques showed only broad, diffuse rings in electron diffraction patterns, for all glasses. The absence of electron diffraction spots or sharp rings and fringes in an orientation suitable for resolution of lattice fringes, using a rotation of sample

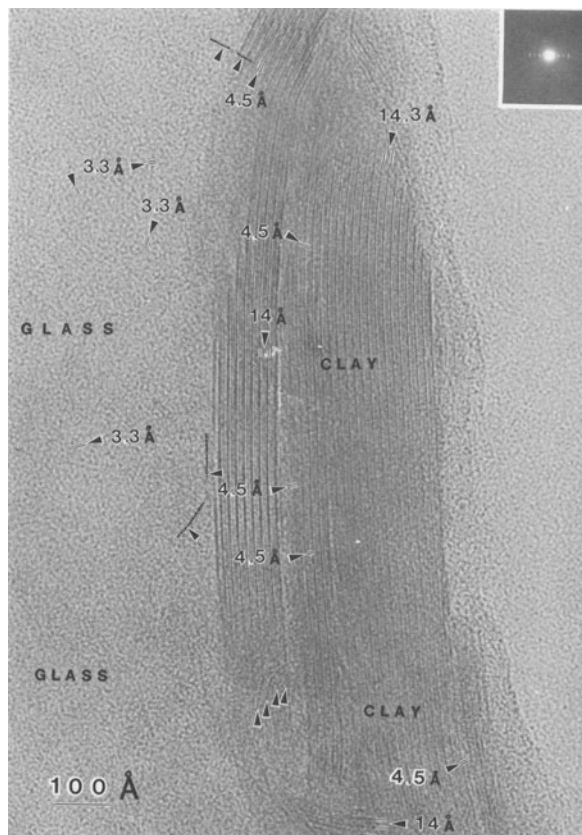


Figure 5. High-resolution transmission electron micrograph showing slightly curved $14\text{-}\text{\AA}$ structure. Note many $3.3\text{-}\text{\AA}$ domain structures in the crystalline region. Curved and spherical structures are preserved in the lower part of illustration.

holder, was taken as sufficient evidence to indicate a glass. The absence of fringes was by itself not sufficient to categorize a material as a glass, if the crystal was not in a proper orientation to produce lattice fringes.

RESULTS

Volcanic glass

HRTEM studies of the sample revealed ordered clusters or domains in about 30% of the fragments. The domains as imaged by HRTEM showed short-range

Table 1. Chemical analyses of volcanic glass and primitive clay phases from energy-dispersive X-ray spectra.

| Elem-line | K-factor | Primitive clays (wt. %) | | | |
|---------------|----------|-------------------------|--------|--------|--------|
| | | Fresh glass (wt. %) | | | |
| Si-K α | 1.000 | 80.22 | 56.01 | 48.19 | 46.90 |
| Al-K α | 1.205 | 14.95 | 8.33 | 4.56 | 4.44 |
| K-K α | 0.914 | 0.67 | 0.62 | 0.56 | 0.55 |
| Ca-K α | 0.890 | 2.74 | 2.50 | 2.19 | 2.13 |
| Ti-K α | 0.983 | 0.86 | 0.60 | 0.53 | 0.52 |
| Fe-K α | 1.084 | 0.57 | 31.94 | 43.97 | 42.79 |
| Mg-K α | 1.484 | 0.00 | 0.00 | 0.00 | 2.68 |
| Total | | 100.01 | 100.00 | 100.00 | 100.01 |

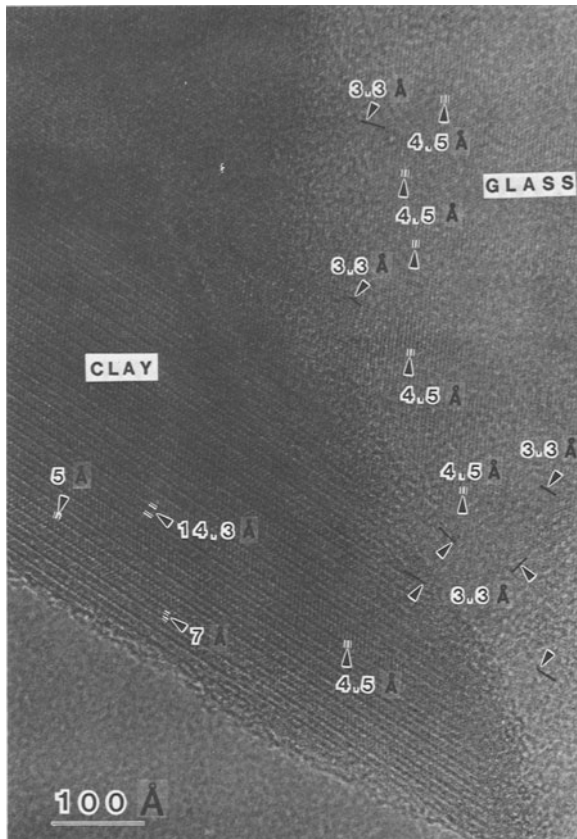


Figure 6. High-resolution transmission electron micrograph showing 3.3- and 4.5-Å domain structures and a well-developed clay phase showing 14.3-Å layer structures.

order having a 3-Å spacing. The glass phase produced typical, broad diffuse rings in electron diffraction patterns.

Small regions within the truly noncrystalline glass matrix showed well-ordered domains having 3–3.3-, 5-, 7-, 8-, and 10-Å spacings (Figures 1 and 2). The domains having 3-Å spacings were generally irregularly distributed, whereas domains having 7-, 8-, and 10-Å layers were curved and formed spherical structures. Three to five concentric layers could be resolved in a domain of about 150-Å diameter (Figure 2). Structures similar to the hollow-packed spheres, having external diameters ranging from 50 to 1000 Å, have been described as precursors to crystalline clay minerals during the hydration of feldspar (Eggleton, 1987). Walls of the hollow-packed spheres showed concentric 3-Å lattice images. Some domains having sets of 10- and 13-Å spacings also contained regular fringes having a 3.3-Å separation. Well-ordered materials having 14- and 16.7-Å spacings were observed on surfaces and well-developed hollow spheres, typically 100–200 Å in diameter, and displayed duplicate to quintuplicate 14- and 19–20-Å lattice images (Figure 3). The electron diffraction patterns suggest a random orientation of

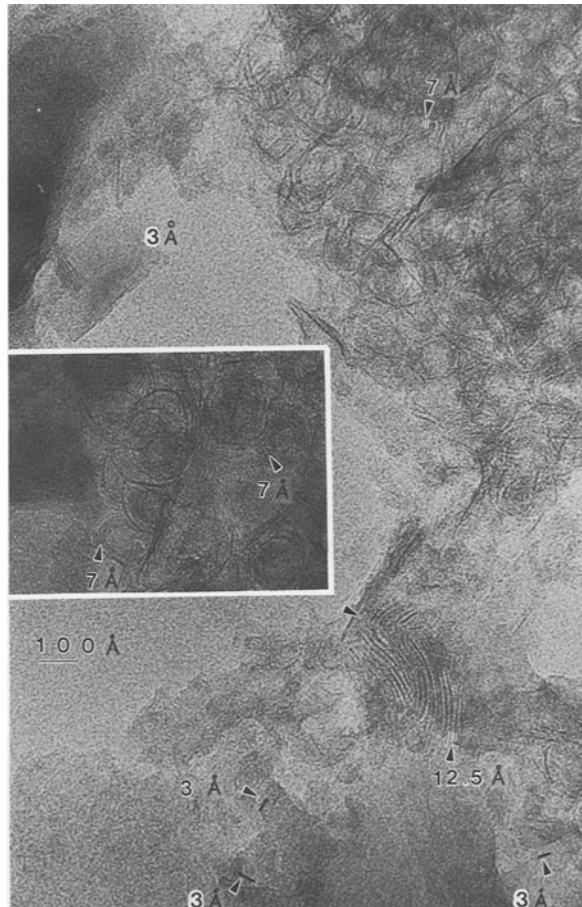


Figure 7. High-resolution transmission electron micrograph of primitive clays on K-feldspar (alkaline igneous complex) showing 7-Å lattice images on sphere walls and curved layer structure having 12.5- and 3-Å domain structure.

these structures. Such well-developed fiber forms showing circular structures are herein designated as “primitive clays”.

Energy-dispersive X-ray analyses (EDX) of the glass phase, the crystalline region, and the primitive clays are shown in Figure 4 and Table 1. The glass phase contained only a small amount of Fe, whereas Fe increased progressively to a maximum in more highly weathered products that showed well-developed hollow spheres of primitive clays (Figure 3). The K, Ca, Ti, and Mg contents of the glass phase remained unchanged, whereas the Si and Al contents of the glass phase were depleted.

Figure 5 shows a 14-Å clay in a fragment as a thin strip parallel to the edge of the particle. The electron diffraction pattern inset shows phyllosilicate diffraction spots at 14.6, 7.0, 4.75, 3.58, and 2.92 Å, suggesting the 001, 002, 003, 004, and 005 spacings of a chlorite-like structure. The lattice images of 4.5 Å (02,11) were also noted in both the crystallite regions and in the clay phases. Curved and spherical structures can be seen at

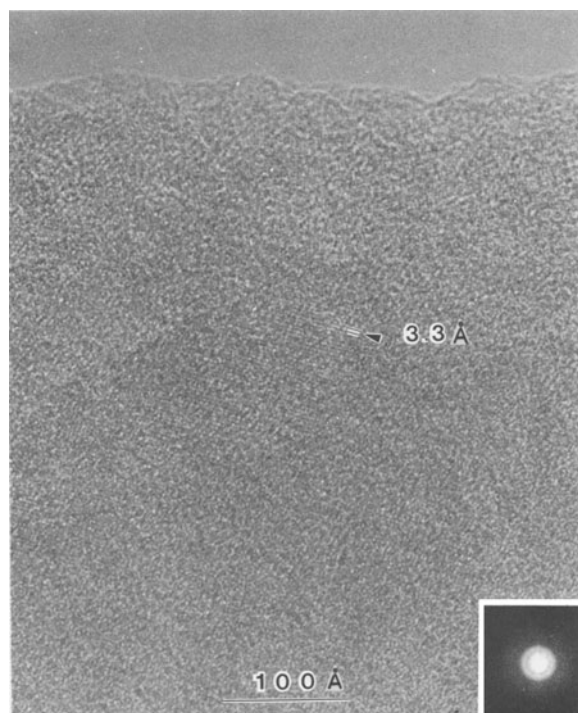


Figure 8. High-resolution transmission electron micrograph of synthetic waste-form glass showing 3.3-Å domain structure in the truly noncrystalline glass matrix and accompanying optical diffraction pattern.

the top and bottom of Figure 5 and may represent some sort of inherited structure. The 3.3-Å domain structures in the crystallite regions were noted in several orientations (left side of Figure 5).

The 4.5-Å domain structure coexisted with the 3.3-Å domain structure next to the clay phase having 14.3-Å spacings (Figure 6). In the well-developed 14.3-Å clay phase, the curved and spherical structures of Figure 5 were not noted. The 4.5-Å spacing in the clay phase appeared to be parallel to 4.5-Å domain structures in the crystallite regions (Figure 6).

Alkalic igneous glass

The HRTEM observations showed a 3-Å domain structure in the crystallite regions (Figure 7) of these rocks, as well as well-developed fibers and circular structures, which showed a 7-Å spacing on K-feldspar in the top right corner of the illustration. A curved layer structure having spacings of 12.5 Å can also be seen in Figure 7. The same curved layer structure was noted in the volcanic glass described above. The circular structures (also in the volcanic glass), about 150-Å in diameter, contained duplicate to quintuplicate 7-Å lattice images (center of Figure 7). The concentration of Si and Al tended to decrease and of Fe to increase from unaltered to altered glass (i.e., primitive clays).

Nuclear-waste-form glass

The nuclear-waste-form glass also showed domain structures (Figure 8) even after two episodes of fusion and annealing for 3 hr at 550°C. The domains as imaged by HRTEM showed short-range order with a 3.3-Å spacing. These crystallite regions (more than a few hundred Ångstroms) were noted within the truly noncrystalline glass matrix. The XRD pattern of this material was characterized by a mid-point hump at 3.3 Å.

Low-angle X-ray powder diffraction

Low-angle XRD measurements of the volcanic and alkalic igneous glass made at controlled relative humidities (RH) of 100%, 50%, and 0% are shown in Figure 9. The pattern of volcanic glass shows major low-angle reflections at 8.5-, 14.6-, and 30-Å, which are consistent with the curved layer structures and 14-Å lattice images obtained by HRTEM (Figure 9a). The background of the low-angle patterns increased with increasing angle, suggesting that the low-angle humps overlapped partly with the large 3.8-Å hump caused by the domain structures.

The low-angle XRD patterns of materials from the alkaline igneous complex (samples 3 and 4, Figures 9B and C, respectively) showed a reflection at about 15.5 Å at 100% RH and 50% RH and a 19-Å reflection at 0% RH. The intensity of the reflections increased with decreasing RH.

A 7.24-Å reflection was clearly evident in the XRD pattern of sample 4 (Figure 9C), which correlates with the duplicate to quintuplicate concentric 7-Å lattice images found by HRTEM (Figure 7).

DISCUSSION

HRTEM permitted the direct visualization of crystal structures to a resolution of about 2-Å range. The present HRTEM and low-angle XRD results showed many kinds of spacings (summarized in Figure 10). All three types of glass revealed crystallite regions showing 3-Å domain structures within the truly noncrystalline glass matrix. Some regions contained both 3- and 4.5-Å domain structures, whereas others had sets of 10- and 13-Å spacings with regular fringes at 3.3-Å separation (Figures 10A–10D).

The primitive clays (Figure 10D) in local domains showed the same general trend in Si, Al, and Fe as described for clay formation on K-feldspar by Tazaki and Fyfe (1987b). Together, the chemical and electron microscope results suggest basic chemical changes within the glass resulting in the localized formation of primitive clays. Only Fe appears to have been significantly enriched in the primitive clay phase, suggesting some substitution of OH and Fe for Ca, K, and other trace elements during the replacement processes. Well-ordered materials having 14- and 16.7-Å spacings were also observed in these regions as thin strips parallel to

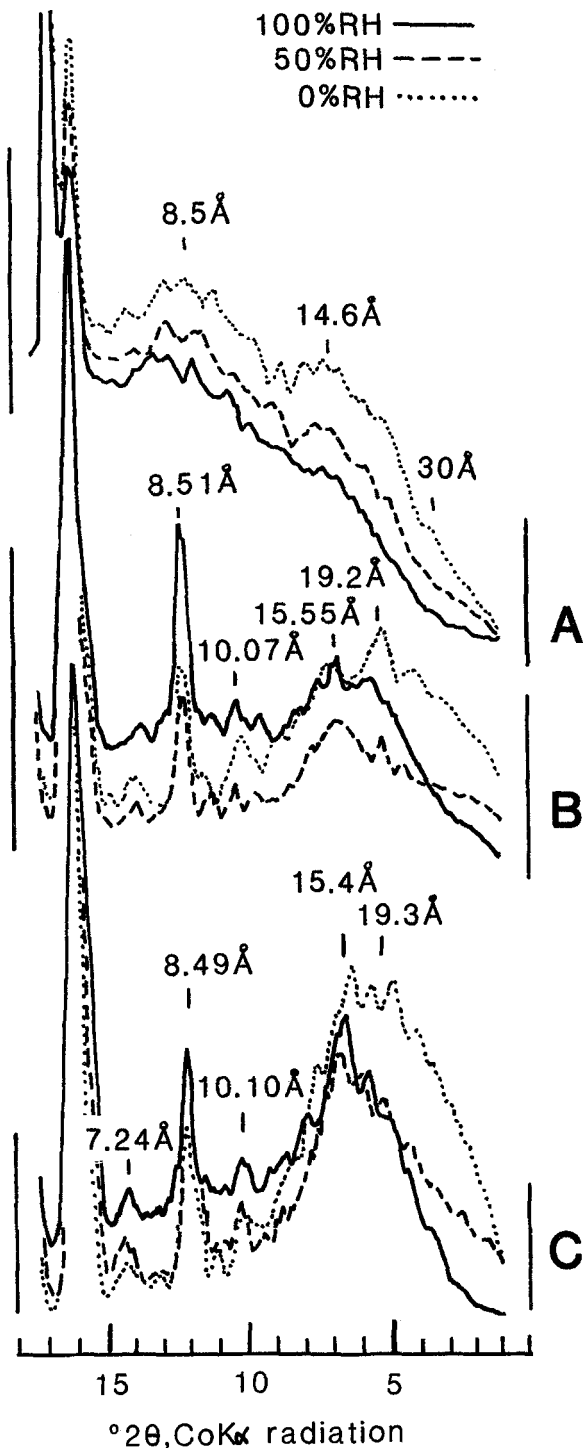


Figure 9. Low-angle X-ray powder diffraction patterns of (A) volcanic glass, (B, C) alkalic igneous glass (samples 3 and 4) showing major reflections at 8.5, 15–19, and 30 Å, related to curved and spherical structures. RH = controlled relative humidities of 100% (solid line), 50% (dashed line), and 0% (dotted line).

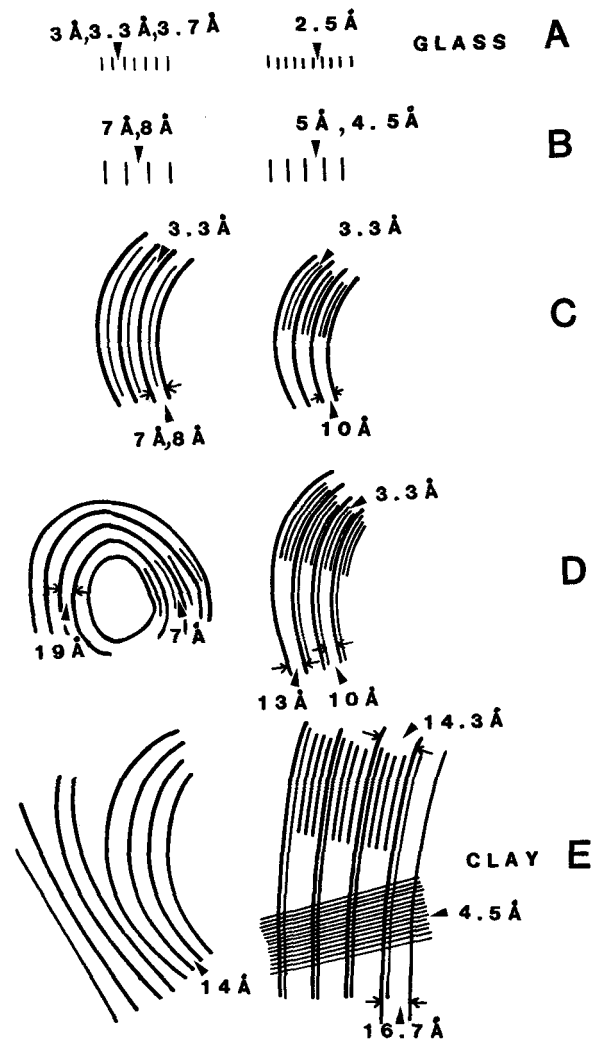


Figure 10. Schematic drawing showing domain structures (A and B), curved structures (C), primitive clays (D), and clay phases (E), which were observed by high-resolution electron microscopy.

the edge of the fragment (Figure 10E). The broad enhancement at 3–3.3 Å demonstrated by XRD (Zarzycki, 1977) may be attributed to the neighboring Si–O or (Si,Al) pairs (Okano *et al.*, 1987) of the glass matrix. These observations of domain structures, the localized lattice images, and the primitive clays found in these natural and synthetic glasses may contribute to an understanding of the growth of clay minerals, and may suggest inherent processes of deterioration of the glasses themselves. It appears that such domains can trigger the growth of clay products on glass substrates.

ACKNOWLEDGMENTS

We thank the staff of JEOL in Tokyo for allowing us to use the JEM 4000FX instrument, and H. C. Palmer and Z. Zhou (University of Western Ontario) for

providing volcanic glass and nuclear-waste-form glass samples.

REFERENCES

- Eggleton, R. A. (1987) Noncrystalline Fe-Si-Al-oxyhydroxides: *Clays & Clay Minerals* **35**, 29–37.
- Eggleton, R. A. and Buseck, P. R. (1980) High-resolution electron microscopy of feldspar weathering: *Clays & Clay Minerals* **28**, 173–178.
- Eggleton, R. A. and Keller, J. (1982) The palagonitization of limburgite glass—A TEM study: *N. Jb. Miner. Mh. Jg. H* **7**, 321–336.
- Kronberg, B. I., Tazaki, K., and Melfi, A. J. (1987) Detailed geochemical studies of the initial stages of weathering of alkaline rocks; Ilha de São Sebastiao, Brazil: *Chemical Geology* **60**, 79–88.
- Okano, M., Marumo, F., Morikawa, H., Nakashima, S., and Iiyama, J. T. (1987) Structures of hydrated glass in the albite-anorthite-quartz system: *J. Mineral.* **13**, 434–442.
- Palmer, H. C., Tazaki, K., Fyfe, W. S., and Zhou, Z. (1988) Precambrian glass: *Geology* **16**, 221–224.
- Tazaki, K. (1976) Clay mineralization of plagioclase: *Earth Science (Chikyū Kagaku) J. Asso. Geological Collaboration in Japan* **30**, 1–3 (in Japanese).
- Tazaki, K. (1978) Micromorphology of plagioclase surface at incipient stage of weathering: *Earth Science (Chikyū Kagaku) J. Asso. Geological Collaboration in Japan* **32**, 58–62 (in Japanese).
- Tazaki, K. (1979) Micromorphology of halloysite produced by weathering of plagioclase in volcanic ash: in *Proc. Int. Clay Conf., Oxford, 1978*, M. M. Mortland and V. C. Farmer, eds., Elsevier, Amsterdam, 415–422.
- Tazaki, K. (1986) Observation of primitive clay precursors during microcline weathering: *Contrib. Mineral. Petrol.* **92**, 86–88.
- Tazaki, K. and Fyfe, W. S. (1985) Discovery of “primitive clay precursors” on alkali-feldspar: *Earth Science (Chikyū Kagaku) J. Asso. Geological Collaboration in Japan* **39**, 443–445 (in Japanese).
- Tazaki, K. and Fyfe, W. S. (1987a) Formation of primitive clay precursors on K-feldspar under extreme leaching conditions: in *Proc. Int. Clay Conf., Denver, 1985*, L. G. Schultz, H. van Olphen, and F. A. Mumpton, eds., The Clay Minerals Society, Bloomington, Indiana, 53–58.
- Tazaki, K. and Fyfe, W. S. (1987b) Primitive clay precursors formed on feldspar: *Canadian J. Earth Sciences* **24**, 506–527.
- van der Gaast, S. J. and Vaars, A. J. (1981) A method to eliminate the background in X-ray diffraction patterns of oriented clay mineral samples: *Clays & Clay Minerals*, **16**, 383–393.
- van der Gaast, S. J., Mizota, C., and Jansen, J. H. F. (1986) Curved smectite in soils from volcanic ash in Kenya and Tanzania: A low-angle X-ray powder diffraction study: *Clays & Clay Minerals*, **34**, 665–671.
- Zarzycki, J. (1977) Structure of non-crystalline inorganic solids: in *Non-Crystalline Solids*, G. H. Frischat, ed., Trans. Tech. Publications, Aedermannsdorf, Switzerland, 52–64.
- Zhou, Z., Fyfe, W. S., and Tazaki, K. (1987) Glass stability in the marine environment: in *Proc. Int. Conf. Natural Analogues in Radioactive Waste Disposal, Brussels, 1987*, B. Côme and N. A. Chapman, eds., Graham & Trotman, London, 153–164.

(Received 8 September 1988; accepted 10 December 1989; Ms. 1826)